ACS OMEGA

http://pubs.acs.org/journal/acsodf

Article

MiR-199 Reverses the Resistance to Gemcitabine in Pancreatic Cancer by Suppressing Stemness through Regulating the Epithelial−Mesenchymal Transition

Weitian Wei, Liang Wang, Liwei Xu, Jinxiao Liang, and Lisong Teng*

Cite This: *ACS Omega* 2021, 6, 31435−31446

Read Online

ACCESS | Metrics & More | Article Recommendations

ABSTRACT: Purpose: the present study aims to investigate the function of miR-199 on gemcitabine (GEM)-resistance in pancreatic cancer, as well as the underlying mechanism. Methods: the GEM-resistant SW1990 cell line (SW1990/SZ) was established. The CCK-8 assay was used to detect the cell viability. The self-renewal of SW1990/SZ cells was evaluated by sphere formation and the colony formation assay. The apoptosis was detected by flow cytometry and the migration ability was measured by the transwell assay. The dual-luciferase gene reporter assay was utilized to confirm the binding between miR-199 and Snail. The expression level of CD44, ALDH1, Nanog, E-cadherin, Vimentin, β-catenin, and Snail was determined by the Western blotting assay. Results: the cell sphere formation rate, number of spheres, and expression level of CD44, ALDH1, and Nanog in GEM-treated SW1990/SZ cells were significantly suppressed by miR-199, accompanied by declined proliferation ability, an increased apoptotic rate, inhibited migration ability, and suppressed EMT progression. The binding site between miR-199 and 3′-UTR of Snail was predicted and confirmed. The inhibitory effect of miR-199 on self-renewal of SW1990/GZ cells and the faciliating property of miR-199 on the inhibitory effect of GEM against the proliferation ability, migration ability, and EMT progression were abolished by overexpressing Snail. Conclusion: MiR-199 reversed the resistance to GEM in pancreatic cancer by suppressing stemness through regulating the EMT.

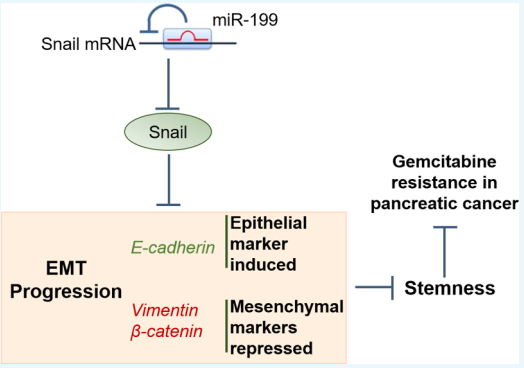

INTRODUCTION

Pancreatic cancer is one of the top three inducements of death from gastrointestinal malignancies in China.[1] It is reported that in 2017, approximately 40,000 patients died of pancreatic cancer in America[2] and 56,000 new patients were diagnosed with pancreatic cancer in 2018, the 5-year relative survival rate of which is only 8%.[3] It is predicted that in 2025, pancreatic cancer will become the second malignancy to induce death, ranking only second to lung cancer.[4] Currently, the main strategies for the treatment of pancreatic cancer are surgery, radiotherapy, and chemotherapy.[5] Since 1997, gemcitabine (GEM) has been used as the first-line treatment for pancreatic cancer due to its higher median survival time than 5-fluorouracil.[6] However, as the consecutive administration of GEM, significant drug resistance is observed.[7] As the resistance mechanism of GEM is currently unclear, rare specific treatment is effective for the treatment of GEM-resistant pancreatic cancer.

Recently, intrinsic resistance has been reported to be widely observed in tumor stem cells[8] and to be responsible for the declined apoptotic rate, decreased mitotic rate, and increased tolerance against DNA injuries.[9−11] It is reported that the chemotherapy resistance and radiation resistance can be induced by tumor stem cells in pancreatic cancer.[12,13] After the treatment of GEM, the proliferation of $CD133^+$ tumor stem cells is suppressed. However, the apoptosis of $CD133^-$ tumor stem cells is not induced. The growth of tumor cells is significantly facilitated after the withdrawal of GEM and the majority of proliferated cells are $CD133^-$-differentiated cells, indicating that the screening and enrichment of tumor stem cells could be induced by the treatment of GEM.[14−16] $CD44^+CD24^+ESA^+$ pancreatic cancer cells are reported to show significant resistance against GEM and radiation.[17] Majority tumor cells could be killed by the treatment of GEM. However, the remaining $CD44^+$ and $CD44^+CD24^+ESA^+$ pancreatic cancer cells will be enriched, which contributes to the relapse and metastasis of pancreatic cancer.[12] In addition, it is reported that the side population (SP) cells possess the characteristics of tumor stem cells, which have been proved to

Received: June 5, 2021
Accepted: August 4, 2021
Published: November 17, 2021

show resistance against GEM.[18] Therefore, targeting tumor stem cells might be an effective method for the treatment of GEM-resistant pancreatic cancer.

Epithelial mesenchymal transition (EMT) is an important process involved in the development of multiple types of malignant tumors, and is reported to be closely related to the maintenance of tumor stem cells and the progressing of chemotherapy resistance.[19] Recently, it has been reported that significant changes in the expression profile of miRNAs are observed in tumor stem cells and multiple miRNAs have been identified to be involved in the regulation of the expression of stem cell biomarkers.[20] A recent report claimed that miR-199 suppressed the processing of EMT by targeting Snail protein.[21] The present study will explore the significant role that miR-199 plays in the process of GEM-resistance against pancreatic cancer by investigating the regulatory effect of miR-199 on EMT progress.

MATERIALS AND METHODS

Agents, Cell Lines, and Treatments. GEM was obtained from Sigma-Aldrich (Missouri, USA). The human pancreatic cancer cell line SW1990 cells were purchased from ATCC (Maryland, USA) and cultured in the Dulbecco's modified Eagle's medium (DMEM) containing 10% fetal bovine serum (FBS) at 37 °C and 5% CO_2.

Establishment of GEM-Resistant Pancreatic Cancer Cell Line (SW1990/GZ). SW1990 cells were seeded on 6-well plates at a density of 5×10^4/mL, followed by incubation for 48 h. After adding different concentrations of GEM into the culturing medium, SW1990 cells were incubated for 1 week for observation. The initial concentration of GEM was settled as IC50 (0.08 μg/mL) derived from the above incubation and CCK-8 assay. Subsequently, SW1990 cells at the exponential phase were incubated with GEM at the concentration of IC50 for 24 h, followed by replacing with the cultural medium without GEM. After entering the exponential phase, SW1990 cells were incubated with GEM at the concentration of 2-fold IC50 for 24 h following twice passages. The above procedures were repeated using the exponentially increasing concentration of GEM successively until the final concentration reached around 1000 μg/mL. Then, treated SW1990 cells were incubated in the GEM-free medium for another 3 months, followed by the CCK-8 assay for verification.

CCK-8 Assay. A CCK-8 assay kit (Jiangcheng, Nanjing, China) was used to detect the cell viability of SW1990 cells and SW1990/GZ cells according to the instruction of the manufacturer. In brief, cells were seeded on 96-well plates, followed by adding 10 μL CCK-8 solution in each well. After incubation at 37 °C for 3 h, the absorbance at 450 nm was detected utilizing a PerkinElmer microplate reader (PerkinElmer, Massachusetts, USA). The concentration−cell viability curve was illustrated and the IC50 value was calculated. The resistant index (RI) was calculated according to the following formula: $RI = IC50_{SW1990/GZ}/IC50_{SW1990}$.

Sphere Formation Assay. SW1990 cells and SW1990/GZ cells at the exponential phase were digested with 0.25% trypsin and centrifugated at 800 rpm for 5 min, followed by resuspending with PBS buffer. After cell counting, 1000 cells were seeded in the 6-well plates containing serum-free DMEM-F12 medium, followed by incubation for 7 days. Finally, a transparent tape with mesh was overlaid on the bottom of the wells and the number of stem cell sphere was counted under an inverted microscope (JEOL, Tokyo, Japan).

Colony Formation Assay. Cells were seeded in 6-well plates at a density of 2×10^2 per well, followed by cultivation in complete media for 10−14 days. Subsequently, medium was removed, cells were washed twice in PBS and were fixed and stained with 6% (v/v) glutaraldehyde and 0.5% crystal violet (Sigma-Aldrich, Missouri, USA) for 60 min at room temperature. Plates were washed with water and air-dried at room temperature.

Flow Cytometry for Apoptosis Analysis. Briefly, cells were seeded in 6-well plates, followed by incubating with 195 μL Annexin V-fluorescein isothiocyanate (Beyotime, Shanghai, China). After adding 5 μL propidium iodide, cells were incubated for 10 min in the dark at room temperature, followed by flow cytometry analysis (BD Biosciences, New Jersey, USA).

Transwell Assay. In brief, cells were collected, counted, and seeded into the transwell insert (Corning, New York, USA) at a density of 1.5×10^5 per well for the migration assay. The lower chamber was filled with medium containing 20% FBS. Cells were then cultured in serum-free medium in the upper chamber for 24 h at 37 °C and 5% CO_2, followed by wiping off cells from the upper chambers. Subsequently, cells from the lower chambers were stained with crystal violet and counted under an optical microscope (JEOL, Tokyo, Japan).

Western Blot Assay. After extracting the total proteins from cells with the RIPA Lysis Buffer (Beyotime, Shanghai, China), the proteins were quantified with a BCA kit (Beyotime, Shanghai, China), followed by being loaded and separated by the sodium dodecyl sulfate−polyacrylamide gel electrophoresis. Then, the separated proteins were transferred to the poly(vinylidene difluoride) membranes (Beyotime, Shanghai, China), followed by incubation with 5% BSA for the removal of non-specific binding proteins. Subsequently, the membrane was incubated with the primary antibody against CD44 (1:1000, CST, Massachusetts, USA), ALDH1 (1:1000, CST, Massachusetts, USA), Nanog (1:1000, CST, Massachusetts, USA), E-cadherin (1:1000, CST, Massachusetts, USA), Vimentin (1:1000, CST, Massachusetts, USA), β-catenin (1:1000, CST, Massachusetts, USA), Snail (1:1000, CST, Massachusetts, USA), and GAPDH (1:1000, CST, Massachusetts, Boston, USA) at 4 °C overnight, followed by being incubated with a secondary antibody at room temperature for 1.5 h. Finally, the membrane was incubated with ECL solution (Beyotime, Shanghai, China), followed by being exposed to Tanon 5200-multi (Tanon, Shanghai, China). Image J software was used to quantify the relative expression level of target proteins.

Cell Transfection. To establish the Snail-overexpressed SW1990/GZ cells, SW1990/GZ cells were transfected with pcDNA3.1-Snail (Genscript, Nanjing, China) and Lipofectamine 2000, followed by incubation for 48 h. The transfection efficacy was determined using the Western blotting assay.

Dual-Luciferase Gene Reporter Assay. The full length 3′-UTR fragment of Snail gene was amplified taking SW1990 cell genome as a template, followed by digesting the PCR product. After ligating the amplified product into pMIR plasmid (Ambion, Texas, USA), the amplified product was transformed into DH5α competent cells (ATCC, Maryland, USA). Following screening the positive clones, the correct sequencing plasmids were picked for transfection, which were named as pMIR-Snail-WT and pMIR-Snail-MUT, respectively. Subsequently, pMIR-Snail-WT or pMIR-Snail-MUT was transfected into HEK293T cells (ATCC, Maryland, USA)

https://doi.org/10.1021/acsomega.1c02945
ACS Omega 2021, 6, 31435−31446

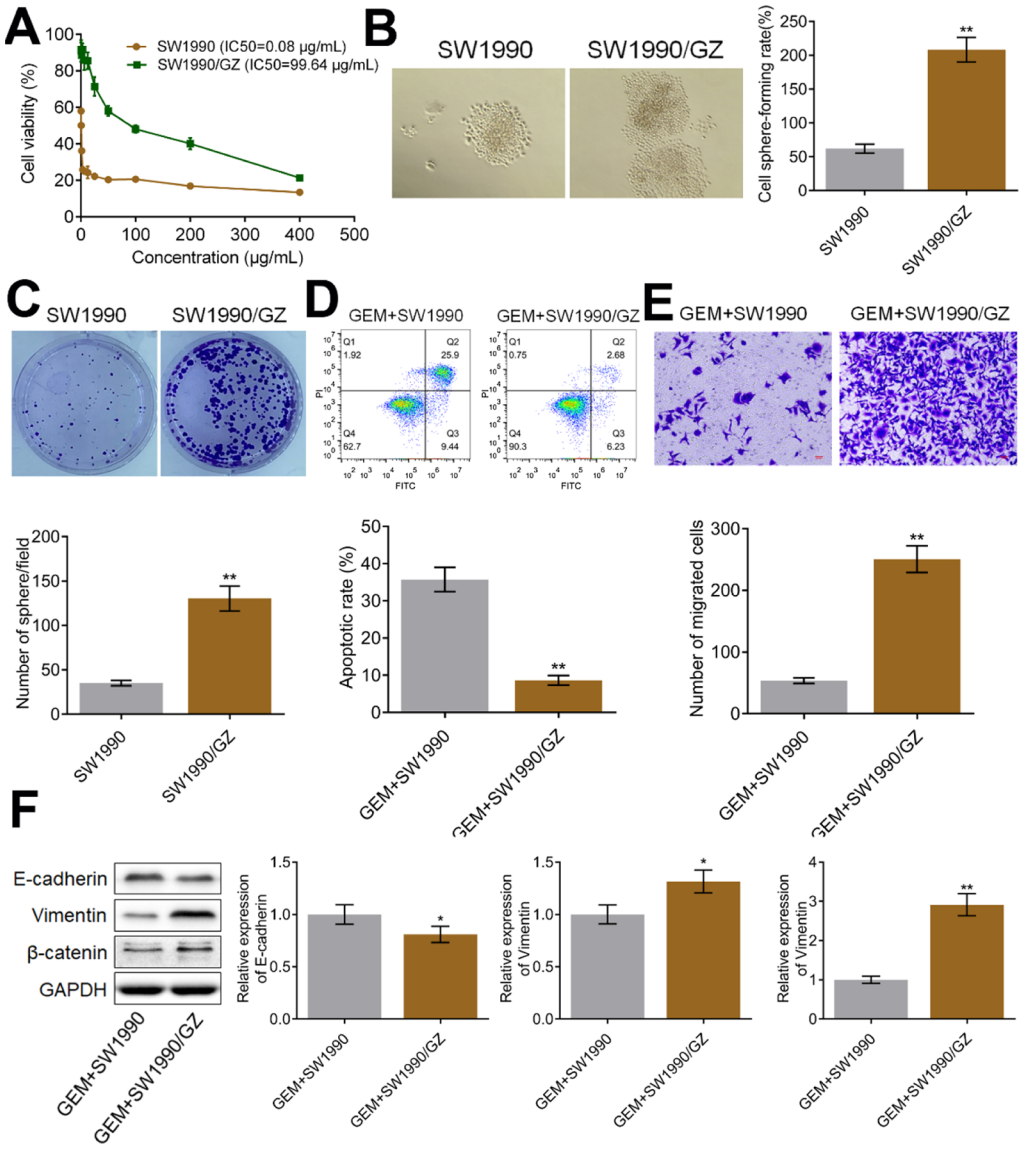

Figure 1. GEM-resistant SW1990 cells (SW1990/GZ cells) were successfully established. (A) Cell viability of SW1990 and SW1990/GZ cells was detected by the CCK-8 assay, and the IC50 values were calculated. (B) Cell sphere formation rate was determined using the sphere formation assay. (C) Number of spheres was counted in the colony formation assay. (D) Flow cytometry was used to measure the apoptosis. (E) Transwell assay was used to determine the migration ability. (F) Expression level of E-cadherin, Vimentin, and β-catenin was determined by the Western blotting assay (*p < 0.05 vs SW1990, **p < 0.01 vs SW1990).

with miR-199 mimic (Genscript, Nanjiang, China) or miR-NC (Genscript, Nanjiang, China) together with Lipofectamine 2000 (Invitrogen, California, USA), followed by 48 h incubation. The relative luciferase activity was detected to follow the instructions of the Dual-Glo Luciferase Assay System Kit (Promega, Wisconsin, USA).

Xenograft Experiments. For the in vivo experiment, five groups were divided: SW1990/GZ, Snail + SW1990/GZ, GEM + SW1990/GZ, miR-199 + GEM + SW1990/GZ, and miR-199 + Snail + GEM + SW1990/GZ groups. Eighteen female BABL/c nude mice were purchased from Charles River Laboratories (Beijing, China). In the SW1990/GZ group, animals were planted with SW1990/GZ cells, followed by intraperitoneal injection with normal saline. In the Snail + SW1990/GZ group, nude mice were planted with Snail-overexpressed SW1990/GZ cells, followed by intraperitoneal injection with normal saline. In the GEM + SW1990/GZ group, animals were planted with SW1990/GZ cells, followed by intraperitoneal injection with 60 mg/kg GEM. Animals in the miR-199 + GEM + SW1990/GZ group were planted with miR-199-transfected SW1990/GZ cells, followed by intraperitoneal injection with 60 mg/kg GEM. Finally, in the miR-199 + Snail + GEM + SW1990/GZ group, nude mice were planted with Snail-overexpressed SW1990/GZ cells, followed by intraperitoneal injection with 60 mg/kg GEM. For each group, three mice were used. All the administrations were initiated until the volume of the tumor reached 100 mm^3. The dosing of GEM was performed on days 1, 4, 7, 10, 14, and 16. The tumor volume was measured and calculated using the formula: $V = L \times W^2/2$, where V represents the volume (mm^3), L represents the greatest diameter (mm), and W represents the lowest diameter (mm). The animals were sacrificed with euthanasia, followed by isolating the tumors for taking pictures and weighing.

https://doi.org/10.1021/acsomega.1c02945
ACS Omega 2021, 6, 31435−31446

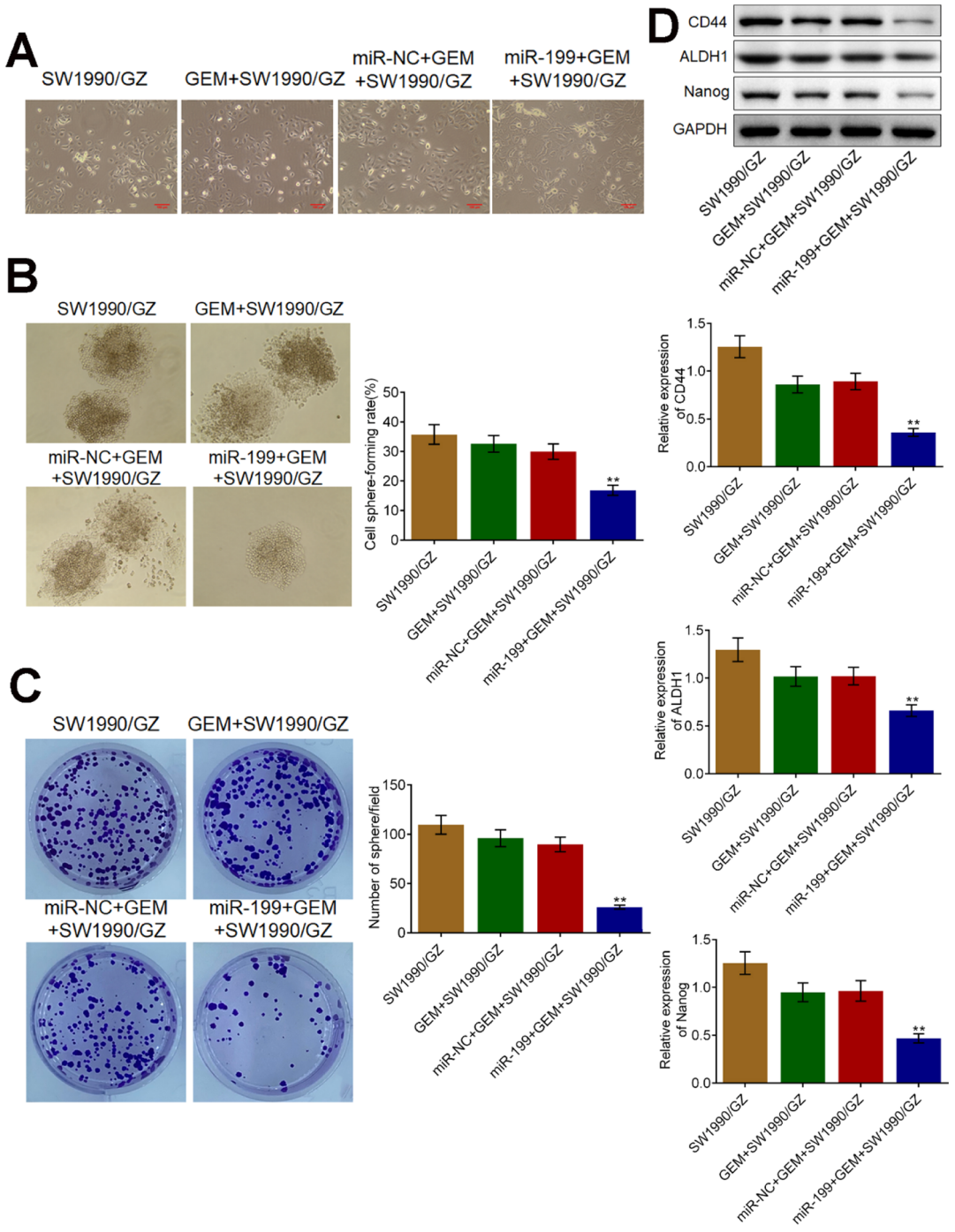

Figure 2. Self-renewal of SW1990/GZ cells was suppressed by miR-199. (A) Morphology of cells was observed under an inverted microscope. (B) Cell sphere formation rate was determined using the sphere formation assay. (C) Number of spheres was counted in the colony formation assay. (D) Expression of CD44, ALDH1, and Nanog was determined by the Western blotting assay (**p < 0.01 vs miR-NC + SW1990/GZ).

Data Analysis. Statistical analyses were performed using t-test or one-way ANOVA. $p < 0.05$ was considered statistically significant. Data are expressed as means ± SD.

RESULTS

GEM-Resistant SW1990 (SW1990/GZ) Cell Line was Successfully Established. To obtain the SW1990/GZ cell line, SW1990 cells were treated with successive doubling concentrations of GEM, followed by detecting the cell viability using the CCK-8 assay. As shown in Figure 1A, compared to SW1990 cells, IC50 of GEM was elevated from 0.08 to 99.64 μg/mL in SW199/SZ cells, with an approximately 1000-fold change. We further compared the self-renewal between SW1990 cells and SW199/SZ cells using the sphere formation assay and colony formation assay. As shown in Figure 1B, compared to SW1990 cells, the cell sphere-forming rate was significantly elevated from 62 to 208 in SW199/SZ cells. The average number of spheres (Figure 1C) in the SW1990 and SW199/SZ group was 35 and 130, respectively (**p < 0.01 vs SW1990). To compare the resistance of SW1990 cells and SW199/SZ cells against the GEM treatment, SW1990 cells and SW199/SZ cells were treated with 0.08 μg/mL GEM, followed

https://doi.org/10.1021/acsomega.1c02945
ACS Omega 2021, 6, 31435−31446

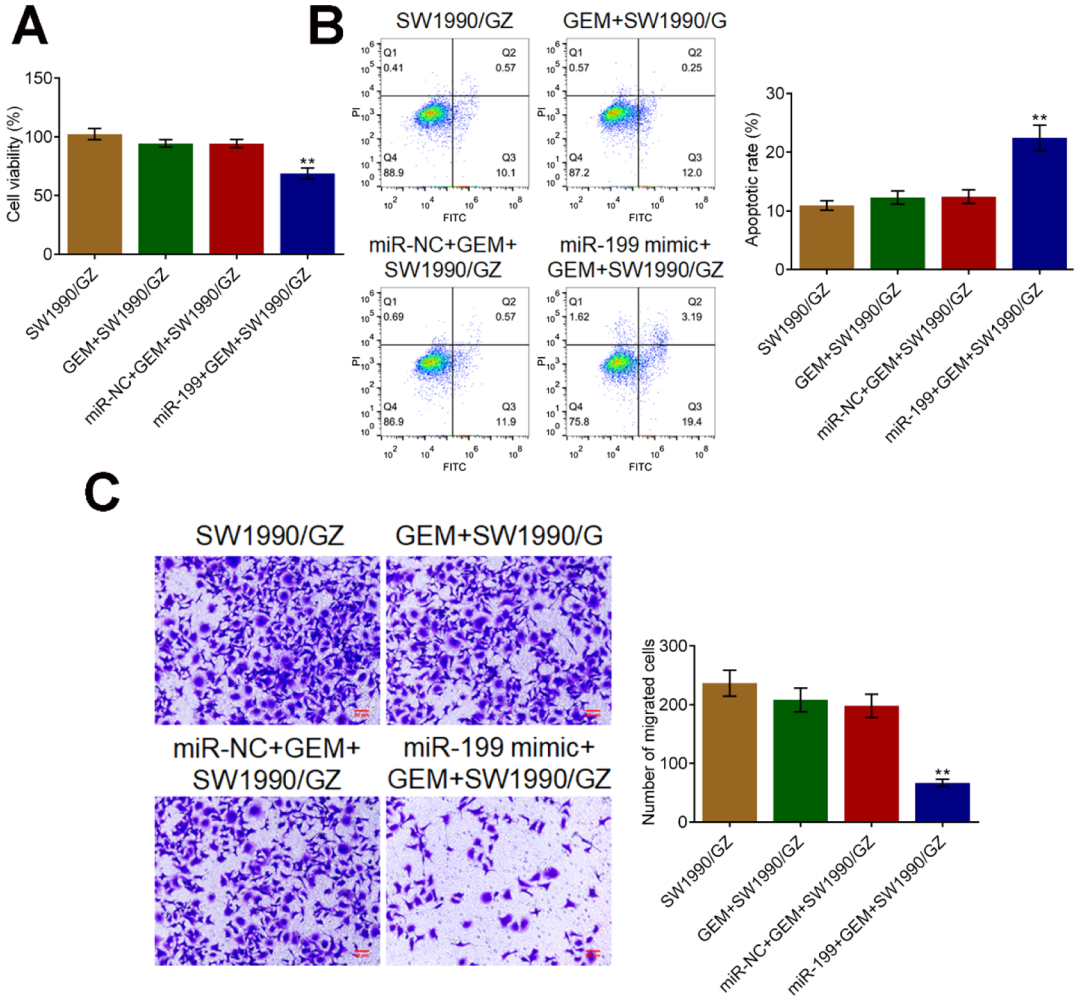

Figure 3. Inhibitory effect of GEM on the proliferation and migration of SW1990/GZ cells was enhanced by miR-199. (A) Cell viability was detected by the CCK-8 assay; (B) tFlow cytometry was used to measure the apoptosis. (C) Transwell assay was used to determine the migration ability (**p < 0.01 vs miR-NC + SW1990/GZ).

by measuring the apoptotic rate, migration ability, and the expression level of EMT proteins. As shown in Figure 1D, compared to SW1990 cells, the apoptotic rate was significantly declined from 35.76 to 8.64% in the SW199/SZ group. The average number of migrated cells (Figure 1E) in the SW1990 and SW199/SZ groups was 54 and 350, respectively (**p < 0.01 vs SW1990). In addition, compared to SW1990 cells, the expression level of E-cadherin was significantly suppressed and the expression level of Vimentin and β-catenin was dramatically elevated in the SW199/SZ group (*p < 0.05 vs SW1990, **p < 0.01 vs SW1990). These data indicate that the GEM-resistant SW1990 (SW1990/GZ) cell line was successfully established.

Self-Renewal of SW1990/GZ was Significantly Suppressed by miR-199. Four groups were divided to evaluate the function of miR-199 in SW1990/GZ cells: SW1990/GZ (SW1990/GZ untreated), GEM + SW1990/GZ (SW1990/GZ cells treated with 0.08 μg/mL GEM), miR-NC + GEM + SW1990/GZ (SW1990/GZ cells treated with 0.08 μg/mL GEM and miR-NC), and miR-199 + GEM + SW1990/GZ (SW1990/GZ cells treated with 0.08 μg/mL GEM and miR-199). The morphology of cells in different groups is shown in Figure 2A. We further evaluated the self-renewal of SW1990/GZ cells using the sphere formation assay and colony formation assay. As shown in Figure 2B, compared to SW1990/GZ, no significant difference in the cell sphere-forming rate was observed in the GEM + SW1990/GZ and miR-NC + GEM + SW1990/GZ groups and the cell sphere-forming rate was dramatically suppressed by the treatment of GEM combined with miR-199 mimic (**p < 0.01 vs miR-NC + SW1990/GZ). In addition, the average number of sphere (Figure 2C) observed in the SW1990/GZ, GEM + SW1990/GZ, and miR-NC + GEM + SW1990/GZ groups was 110, 96, and 90, respectively, which was significantly declined to 26 in the miR-199 + GEM + SW1990/GZ group (**p < 0.01 vs miR-NC + SW1990/GZ). Finally, the expression level of biomarkers of tumor stem cells was determined. As shown in Figure 2D, compared to SW1990/GZ, no significant difference in the expression level of CD44, ALDH1, and Nanog was observed in GEM-treated SW1990/GZ cells. Compared to the miR-NC + GEM + SW1990/GZ group, CD44, ALDH1, and Nanog were dramatically downregulated in the miR-199 + GEM + SW1990/GZ group (**p < 0.01 vs miR-NC + SW1990/GZ). These data indicate that self-renewal of SW1990/GZ was significantly suppressed by the introduction of miR-199 mimic.

Inhibitory Effect of GEM on the Proliferation and Metastasis of SW1990/GZ was Enhanced by miR-199.

https://doi.org/10.1021/acsomega.1c02945
ACS Omega 2021, 6, 31435−31446

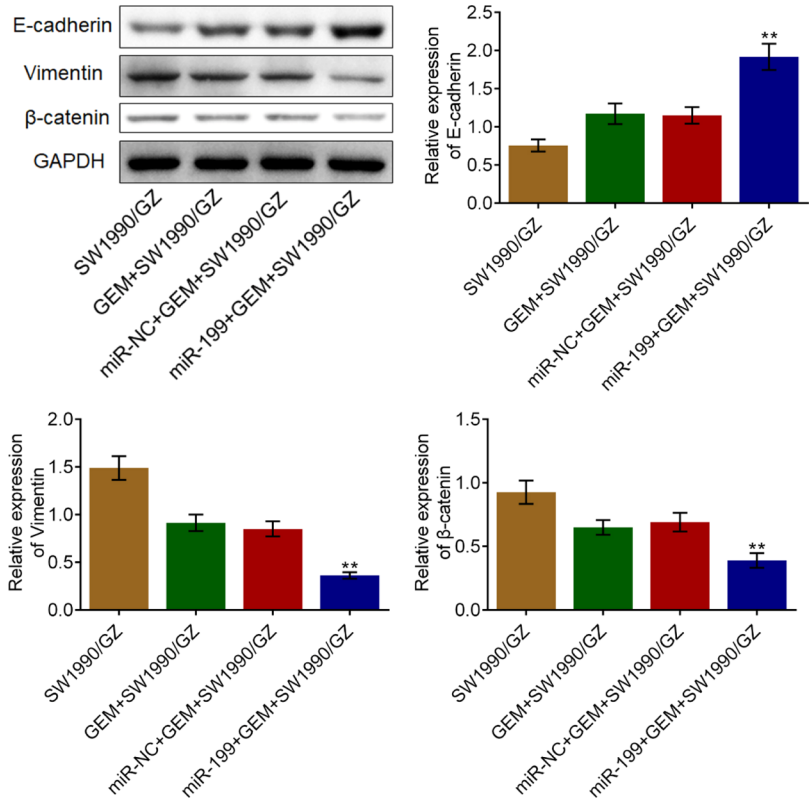

Figure 4. Inhibitory effect of GEM on EMT progression of SW1990/GZ cells was enhanced by miR-199. The expression level of E-cadherin, Vimentin, and β-catenin was determined by the Western blotting assay (**p < 0.01 vs miR-NC + SW1990/GZ).

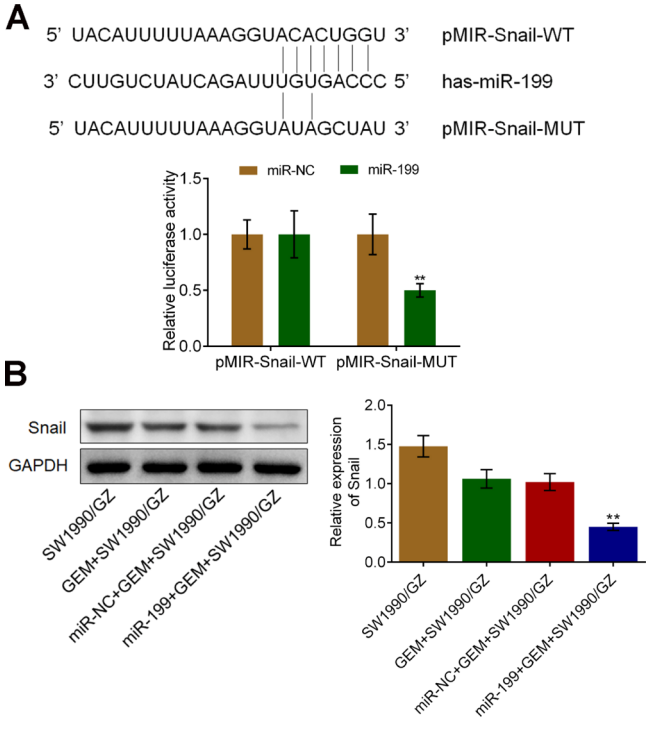

Figure 5. miR-199 targeted Snail to regulate its expression in SW1990/GZ cells. (A) Binding site between miR-199 and Snail was confirmed by the dual-luciferase gene reporter assay (**p < 0.01 vs miR-NC). (B) Expression level of Snail was determined by the Western blotting assay (**p < 0.01 vs miR-NC + SW1990/GZ).

After different treatment strategies, the proliferation and migration ability of treated SW1990/GZ cells were evaluated. As shown in Figure 3A, no significant difference in cell viability was observed between the SW1990/GZ group and the GEM + SW1990/GZ group. Compared to the miR-NC + SW1990/GZ group, cell viability was declined significantly in the miR-199 + GEM + SW1990/GZ group (**p < 0.01 vs miR-NC + SW1990/GZ). In addition, the apoptotic rate in the SW1990/GZ, GEM + SW1990/GZ, and miR-NC + SW1990/GZ groups was 10.95, 12.28, and 12.45%, respectively, which was dramatically suppressed to 22.43% by the treatment of GEM combined with miR-199 mimic (**p < 0.01 vs miR-NC + SW1990/GZ). These data indicate that the inhibitory effect of GEM against SW1990/GZ was significantly enhanced by the introduction of miR-199. As shown in Figure 3C, compared to SW1990/GZ, the number of migrated GEM-treated SW1990/GZ cells was slightly reduced, though without significant difference. Compared to the miR-NC + SW1990/GZ group, the number of migrated GEM and miR-199 mimic-treated SW1990/GZ cells was pronouncedly declined (**p < 0.01 vs miR-NC + SW1990/GZ), indicating that the inhibitory effect of GEM on SW1990/GZ cells was greatly enhanced by miR-199.

Inhibitory Effect of GEM on EMT Progressing of SW1990/GZ was Strengthened by miR-199. We further investigated the progressing of EMT in different groups. As shown in Figure 4, the expression level of E-cadherin was slightly elevated and that of Vimentin and β-catenin was slightly inhibited by the introduction of GEM, though without significant difference. Compared to the miR-NC + SW1990/GZ group, significant elevated expression of E-cadherin and suppressed expression of Vimentin and β-catenin were

https://doi.org/10.1021/acsomega.1c02945
ACS Omega 2021, 6, 31435−31446

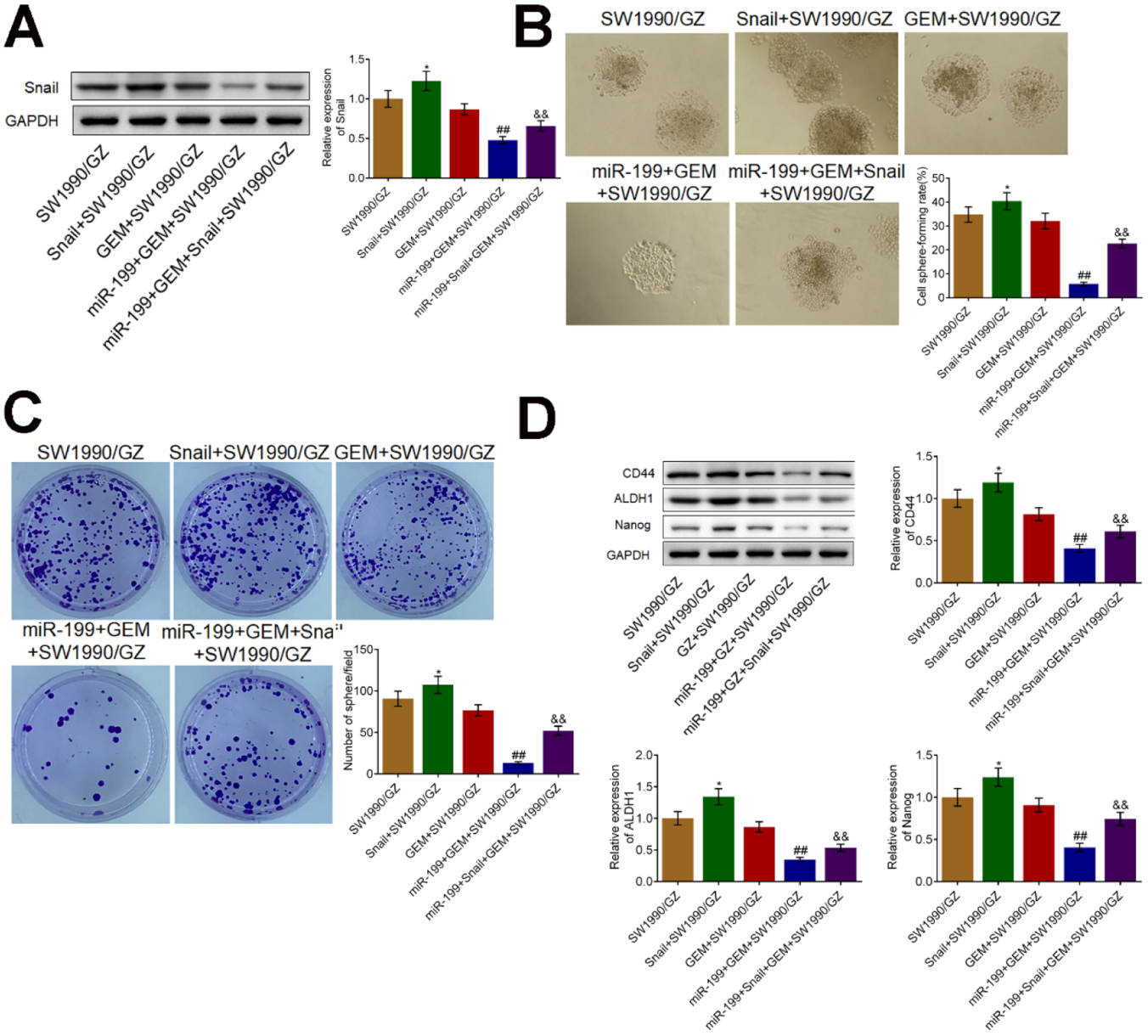

Figure 6. Inhibitory effect of miR-199 on self-renewal of SW1990/GZ cells was abolished by overexpressing Snail. (A) Transfection efficacy was verified by the Western blotting assay. (B) Cell sphere formation rate was determined using the sphere formation assay. (C) Number of spheres was counted in the colony formation assay. (D) Expression of CD44, ALDH1, and Nanog was determined by the Western blotting assay (*p < 0.05 vs SW1990/GZ, ##p < 0.01 vs GEM + SW1990/GZ, and &&p < 0.01 vs miR-199 + GEM + SW1990/GZ).

observed in the miR-199 + GEM + SW1990/GZ group (**p < 0.01 vs miR-NC + SW1990/GZ). These data indicate that the inhibitory effect of GEM on EMT progressing of SW1990/GZ was dramatically strengthened by miR-199.

miR-199-Targeted Snail to Regulate Its Expression in SW1990/GZ Cells. According to the analysis of bioinformatics, a potential binding site for miR-199 within the 3′ UTR of Snail was determined (shown in Figure 5A Upper). To verify that miR-199 was bound with Snail on this site, a reporter vector consisting of a luciferase cDNA, followed by the 3′ UTR of Snail (pMIR-Snail-WT) was constructed and a luciferase reporter vector fused to the Snail 3′ UTR but with a mutant miR-199 response element (pMIR-Snail-MUT) was constructed. pMIR-Snail-WT or pMIR-Snail-MUT was transfected into SW1990/GZ cells. Control or pre-miR-199 was cotransfected into SW1990/GZ cells, and the luciferase activity was detected. The luciferase activity of the reporter vector containing the miR-199 response element was decreased by premiR-199 (Figure 5A, **p < 0.01 vs miR-NC), suggesting that miR-199 suppressed the transcription of Snail mRNA by acting on a response element in the Snail 3′ UTR. We further detected the expression level of Snail using the Western blotting assay, the results of which are shown in Figure 5B. Compared to the miR-NC + GEM + SW1990/GZ group, Snail was found to be significantly downregulated in the miR-199 + GEM + SW1990/GZ group, which verified the regulatory effect of miR-199 on the expression of Snail.

Overexpressing Snail Abolished the Inhibitory Effect of miR-199 on Self-Renewal of SW1990/GZ. To investigate whether the biofunction of miR-199 on tumor stem cells was associated with its target protein Snail, the Snail-overexpressed SW1990/GZ cells were established by trans-

https://doi.org/10.1021/acsomega.1c02945
ACS Omega 2021, 6, 31435−31446

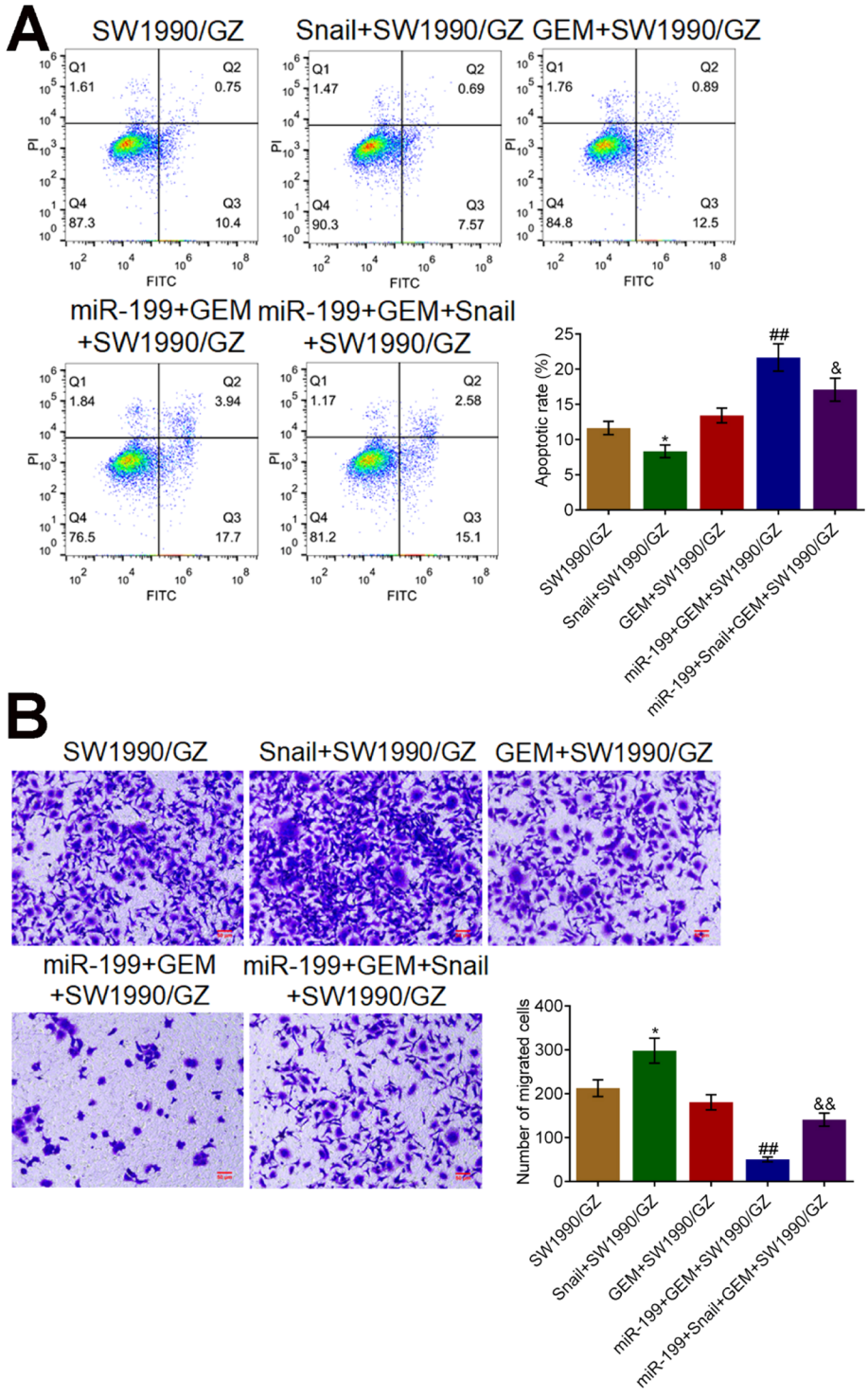

Figure 7. Enhancement of miR-199 on the inhibitory effect of GEM against the proliferation and migration ability of SW1990/GZ cells was abolished by overexpressing Snail. (A) Flow cytometry was used to measure the apoptosis. (C) Transwell assay was used to determine the migration ability (*p < 0.05 vs SW1990/GZ, ##p < 0.01 vs GEM + SW1990/GZ, &p < 0.05 vs miR-199 + GEM + SW1990/GZ, and &&p < 0.01 vs miR-199 + GEM + SW1990/GZ).

fecting cells with pcDNA3.1-Snail plasmids. As shown in Figure 6A, compared to SW1990/GZ, Snail was significantly upregulated in SW1990/GZ cells transfected with pcDNA3.1-Snail plasmids (Snail + SW1990/GZ). As expected, compared to the GEM + SW1990/GZ group, the expression level of Snail was dramatically inhibited in the miR-199 + GEM + SW1990/GZ group, which was further elevated by the transfection of pcDNA3.1-Snail plasmids (miR-199 + GEM + Snail + SW1990/GZ). In addition, compared to SW1990/GZ, the cell sphere-forming rate (Figure 6B) was greatly elevated from 34.8 to 40.4% in the Snail + SW1990/GZ group. Compared to the GEM + SW1990/GZ group, the cell sphere-forming rate was significantly decreased from 32.1 to 5.7% by the additional introduction of miR-199, which was promoted to 22.7% in the

https://doi.org/10.1021/acsomega.1c02945
ACS Omega 2021, 6, 31435−31446

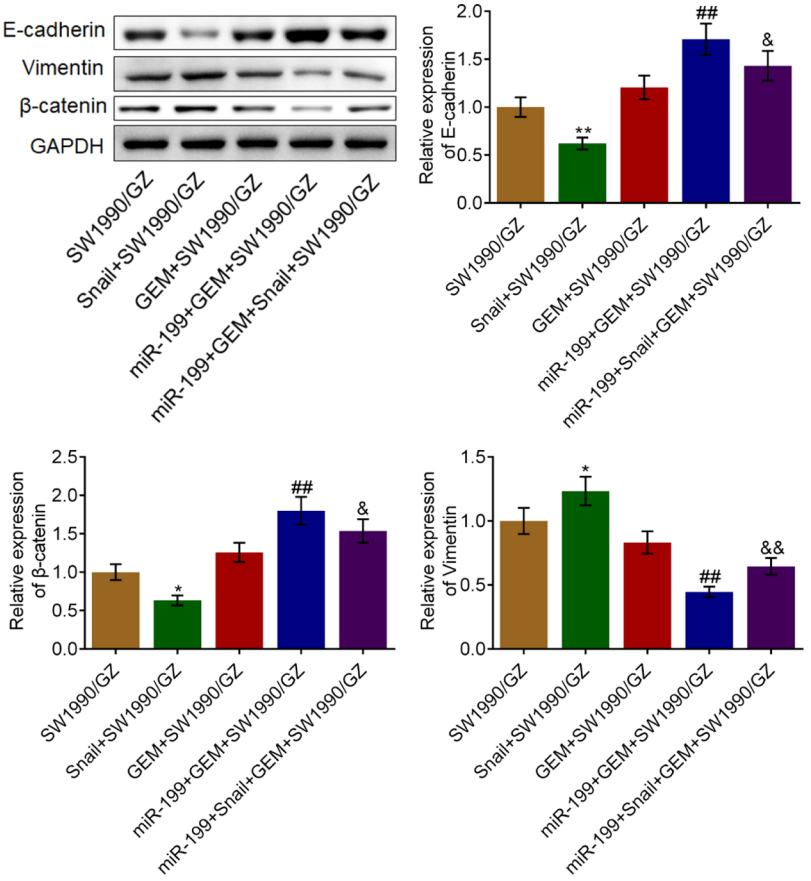

Figure 8. Enhancement of miR-199 on the inhibitory effect of GEM against the EMT progressing of SW1990/GZ cells was abolished by overexpressing Snail. The expression level of E-cadherin, Vimentin, and β-catenin was determined by the Western blotting assay (*p < 0.05 vs SW1990/GZ, ##p < 0.01 vs GEM + SW1990/GZ, &p < 0.05 vs miR-199 + GEM + SW1990/GZ, and &&p < 0.01 vs miR-199 + GEM + SW1990/GZ).

miR-199 + GEM + Snail + SW1990/GZ group. As shown in Figure 6C, the number of sphere in the Snail + SW1990/GZ group was significantly more than that in the SW1990/GZ group. Compared to the GEM + SW1990/GZ group, the number of sphere was significantly declined from 77 to 13 in the miR-199 + GEM + SW1990/GZ group, which was further greatly increased to 52 in the miR-199 + GEM + Snail + SW1990/GZ group. Finally, compared to SW1990/GZ, CD44, ALDH1, and Nanog were significantly upregulated by the overexpression of Snail. Compared to the GEM + SW1990/GZ group, the expression level of CD44, ALDH1, and Nanog was dramatically suppressed by the cointroduction of miR-199, which was further elevated in the miR-199 + GEM + Snail + SW1990/GZ group (*p < 0.05 vs SW1990/GZ, ##p < 0.01 vs GEM + SW1990/GZ, and &&p < 0.01 vs miR-199 + GEM + SW1990/GZ). These data indicate that the inhibitory effect of miR-199 on self-renewal of SW1990/GZ was significantly abolished by overexpressing Snail in SW1990/GZ cells.

Overexpressing Snail Abolished the Enhancement of miR-199 on the Inhibitory Effect of GEM against the Proliferation and Migration Ability of SW1990/GZ Cells. As shown in Figure 7A, compared to SW1990/GZ (incubated in GEM-free medium), the apoptotic rate was significantly declined from 11.64 to 8.32%. Compared to the GEM + SW1990/GZ group, the apoptotic rate was greatly elevated from 13.43 to 21.67% by the additional treatment of miR-199, which was further decreased to 17.1% in the miR-199 + GEM + Snail + SW1990/GZ group. In addition, the average number of migrated cells in the SW1990/GZ, Snail + SW1990/GZ, GEM + SW1990/GZ, miR-199 + GEM + SW1990/GZ, and miR-199 + GEM + Snail + SW1990/GZ groups was 213, 298, 181, 50, and 141, respectively (*p < 0.05 vs SW1990/GZ, ##p < 0.01 vs GEM + SW1990/GZ, &p < 0.05 vs miR-199 + GEM + SW1990/GZ, and &&p < 0.01 vs miR-199 + GEM + SW1990/GZ). These data indicate that the inhibitory effect of GEM against the proliferation and migration ability of SW1990/GZ cells was enhanced by miR-199, which was reversed by overexpressing Snail.

Overexpressing Snail Reversed the Facilitating Property of miR-199 on the Inhibitory Effect of GEM Against the EMT Progressing of SW1990/GZ Cells. We further investigated the progressing of EMT in each group. As shown in Figure 8, compared to SW1990/GZ, the expression of E-cadherin was greatly suppressed and that of Vimentin and β-catenin was greatly promoted in the Snail + SW1990/GZ group. Compared to the GEM + SW1990/GZ group, E-cadherin was significantly upregulated and Vimentin and β-catenin were significantly downregulated by the cointroduction of miR-199, which were reversed in the miR-199 + GEM + Snail + SW1990/GZ group (*p < 0.05 vs SW1990/GZ, ##p < 0.01 vs GEM + SW1990/GZ, &p < 0.05 vs miR-199 + GEM + SW1990/GZ, and &&p < 0.01 vs miR-199 + GEM + SW1990/GZ).

Overexpressing Snail Reversed the Strengthening of miR-199 on the Inhibitory Effect of GEM against in Vivo Tumor Growth of SW1990/GZ Cells. Finally, to verify that

https://doi.org/10.1021/acsomega.1c02945
ACS Omega 2021, 6, 31435−31446

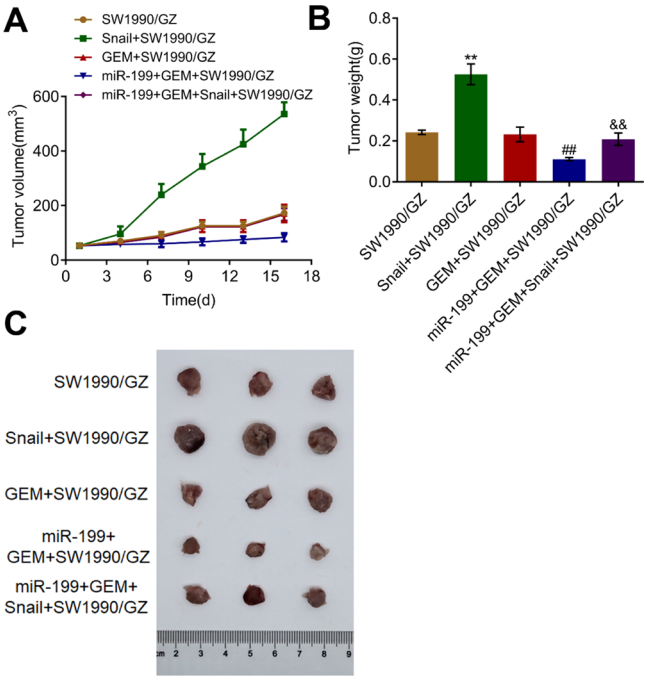

Figure 9. Strengthening of miR-199 on the inhibitory effect of GEM against in vivo tumor growth of SW1990/GZ cells was abolished by overexpressing Snail. (A) Tumor volume was recorded during the treatments on days 1, 4, 7, 10, 14, and 16. (B) Tumor weights were recorded at the end of the animal experiment. (C) Picture of tumors was taken at the end of the animal experiment (**p < 0.01 vs SW1990/GZ, ##p < 0.01 vs GEM + SW1990/GZ, and &&p < 0.01 vs miR-199 + GEM + SW1990/GZ).

the effects of miR-199 on GEM-resistance in SW1990/GZ cells were related to the function of Snail, the xenograft experiment was conducted. As shown in Figure 9, after 16 day treatments, compared to the SW1990/GZ group, the tumor volume and tumor weight were significantly increased in the Snail + SW1990/GZ group (**p < 0.01 vs SW1990/GZ). Compared to the GEM + SW1990/GZ group, the tumor volume and tumor weight were dramatically declined in the miR-199 + GEM + SW1990/GZ, which were greatly reversed in the miR-199 + GEM + Snail + SW1990/GZ group (##p < 0.01 vs GEM + SW1990/GZ, &&p < 0.01 vs miR-199 + GEM + SW1990/GZ).

DISCUSSION

MiRNAs are a group of non-coding RNAs composed of 20−25 base pair sequences, and are involved in the regulation of key tumor-related protein expression. Although only occupying approximately 3% in the total human genome, miRNAs regulate the encoding of 20−30% proteins, which play an important role in regulating the proliferation, metastasis, and drug resistance of tumor cells.[22,23] Recently, it has been widely reported that miRNAs are involved in the regulation of self-renewal of tumor stem cells by mediating the biomarker of tumor stem cells,[24] such as cluster of differentiation-44 (CD44),[25] aldehyde dehydrogenase 1 (ALDH1),[26] and Nanog.[27] It is reported that upregulated expression of miR-34, a tumor suppressor miRNA, inhibits the proliferation of human pancreatic cancer tumor-initiating cells, which indicates that miR-34 is involved in the self-renewal process of pancreatic cancer stem cells.[28,29] Hasegawa reported that the overexpression of miRNA-1246 is related to CCNG2-mediated chemoresistance and stemness in pancreatic cancer.[30] In the present study, the biofunction of miR-199, which is regarded as a tumor suppressor miRNA,[21] in the progressing of pancreatic cancer was investigated. We first established the GEM-resistant pancreatic cancer cells, SW1990/GZ, using the intermittent concentration-gradient multiplication method, which was verified by the 1000-fold increased IC50 of GEM against SW1990/GZ compared to SW1990 cells. After the treatment of miR-199, we found that the self-renewal of GEM-treated SW1990/GZ cells was significantly suppressed, verified by the decreased cell sphere-forming rate, declined number of spheres, and downregulated biomarkers of cancer stem cells. These data revealed that miR-199 might act as a tumor suppressor miRNA by inhibiting the self-renewal process of pancreatic cancer stem cells.

Several reports claimed the important role of pancreatic cancer stem cells in the development of chemotherapy resistance. Yang reported that the drug resistance was significantly enhanced by exosomes derived from cancer stem cells of GEM-resistant pancreatic cancer cells.[31] Zhao claimed that stem-like cell properties in pancreatic cancer could be induced by the treatment of GEM through ROS/KRAS/AMPK signaling.[32] In the present study, after the introduction of miR-199, the inhibitory effect of GEM against the proliferation and migration ability of SW1990/GZ cells was significantly enhanced, indicating that miR-199 might reverse the GEM-resistance against pancreatic cancer by suppressing the self-renewal process of pancreatic cancer stem cells.

The progressing of EMT is reported to be closely related to the stem-like property of both pancreatic normal and neoplastic cells.[33,34] The association between EMT phenotypes and cancer stem cells has recently been investigated in multiple types of malignant tumors, including pancreatic cancer.[35−37] EMT is defined as the transdifferentiation of epithelial cells into motile mesenchymal cells, which is found to be involved in multiple physiological processes, such as wound healing and stem cell behavior.[38] The downregulation of biomarkers of epithelial cells, such as E-cadherin, and the upregulation of biomarkers of motile mesenchymal cells, such as Vimentin and β-catenin, are regarded as signs for the progression of EMT.[39] Protein Snail is an important transcription factor that induces the development of EMT.[40] In the present study, we first found that the inhibitory effect of GEM on EMT in pancreatic cancer cells was significantly suppressed by the introduction of miR-199, which was accompanied by the downregulation of Snail. The specific targeting between miR-199 and Snail was confirmed in the present study using the dual-luciferase reporter assay, which was consistent with the report described previously.[21] Subsequently, the involvement of Snail in the biofunction of miR-199 was further verified by overexpressing Snail in SW1990/GZ cells, followed by introduction of miR-199 and GEM treatment. The results showed that the effects of miR-199 on the self-renewal of SW1990/GZ cells and the antitumor efficacy of GEM were significantly abolished by the overexpression of Snail, indicating that miR-199 reversed the resistance to GEM in pancreatic cancer by downregulating Snail. In addition, the inhibition of EMT progression was accompanied. Finally, the facilitating property of miR-199 on the inhibitory effect of GEM against in vivo tumor growth of SW1990/GZ was proved to be mediated by the inhibition of Snail. In our future work, the upstream regulatory pathway of miR-199 will be further explored to better understand the

https://doi.org/10.1021/acsomega.1c02945
ACS Omega 2021, 6, 31435−31446

mechanism underlying the GEM-resistance during the treatment of pancreatic cancer.

Taken together, our data indicate that miR-199 reversed the resistance to GEM in pancreatic cancer by suppressing stemness through regulating the EMT.

AUTHOR INFORMATION

Corresponding Author

Lisong Teng − *Department of Surgical Oncology, Zhejiang University School of Medicine First Affiliated Hospital, Hangzhou 310009, China*; Email: lsteng@zju.edu.cn

Authors

Weitian Wei − *Department of Surgical Oncology, Zhejiang University School of Medicine First Affiliated Hospital, Hangzhou 310009, China; Department of Surgical Oncology, Zhejiang Cancer Hospital, Hangzhou 310022, China;* orcid.org/0000-0002-9970-2381

Liang Wang − *Department of Surgical Oncology, Zhejiang Cancer Hospital, Hangzhou 310022, China*

Liwei Xu − *Department of Surgical Oncology, Zhejiang Cancer Hospital, Hangzhou 310022, China*

Jinxiao Liang − *Department of Surgical Oncology, Zhejiang Cancer Hospital, Hangzhou 310022, China*

Complete contact information is available at: https://pubs.acs.org/10.1021/acsomega.1c02945

Funding

This work was supported by grants from the Natural Science Foundation of Zhejiang Province (grant no. LQ20H310001).

Notes

The authors declare no competing financial interest.

REFERENCES

(1) Li, H.-Y.; Cui, Z.-M.; Chen, J.; Guo, X.-Z.; Li, Y.-Y. Pancreatic cancer: diagnosis and treatments. *Tumour Immunobiol.* **2015**, *36*, 1375−1384.

(2) *Anonymous, Cancer Facts & Figures 2017*; Cancer Facts & Figures, 2017.

(3) *Anonymous, Cancer Facts & Figures 2018*; Cancer Facts & Figures, 2018.

(4) Matsuno, S.; Egawa, S.; Fukuyama, S.; Motoi, F.; Sunamura, M.; Isaji, S.; Imaizumi, T.; Okada, S.; Kato, H.; Suda, K.; Nakao, A.; Hiraoka, T.; Hosotani, R.; Takeda, K. Pancreatic Cancer Registry in Japan: 20 years of experience. *Pancreas* **2004**, *28*, 219−230.

(5) Brunner, M.; Wu, Z.; Krautz, C.; Pilarsky, C.; Grützmann, R.; Weber, G. F. Current Clinical Strategies of Pancreatic Cancer Treatment and Open Molecular Questions. *Int. J. Mol. Sci.* **2019**, *20*, 4543.

(6) Burris, H. A., 3rd; Moore, M. J.; Andersen, J.; Green, M. R.; Rothenberg, M. L.; Modiano, M. R.; Cripps, M. C.; Portenoy, R. K.; Storniolo, A. M.; Tarassoff, P.; Nelson, R.; Dorr, F. A.; Stephens, C. D.; Von Hoff, D. D. Improvements in survival and clinical benefit with gemcitabine as first-line therapy for patients with advanced pancreas cancer: a randomized trial. *J. Clin. Oncol.* **1997**, *15*, 2403−2413.

(7) Binenbaum, Y.; Na'ara, S.; Gil, Z. Gemcitabine resistance in pancreatic ductal adenocarcinoma. *Drug Resist. Updates* **2015**, *23*, 55−68.

(8) Li, Y.; Kong, D.; Ahmad, A.; Bao, B.; Sarkar, F. H. Pancreatic cancer stem cells: emerging target for designing novel therapy. *Canc. Lett.* **2013**, *338*, 94−100.

(9) Zhu, Y. Y.; Yuan, Z. Pancreatic cancer stem cells. *Am. J. Cancer Res.* **2015**, *5*, 894−906.

(10) Cojoc, M.; Mäbert, K.; Muders, M. H.; Dubrovska, A. A role for cancer stem cells in therapy resistance: cellular and molecular mechanisms. *Semin. Canc. Biol.* **2015**, *31*, 16−27.

(11) Richard, V.; Nair, M. G.; Kumar, T. R. S.; Pillai, M. R. Side population cells as prototype of chemoresistant, tumor-initiating cells. *BioMed Res. Int.* **2013**, *2013*, 517237.

(12) Hong, S. P.; Wen, J.; Bang, S.; Park, S.; Song, S. Y. CD44-positive cells are responsible for gemcitabine resistance in pancreatic cancer cells. *Int. J. Cancer* **2009**, *125*, 2323−2331.

(13) Hermann, P. C.; Huber, S. L.; Herrler, T.; Aicher, A.; Ellwart, J. W.; Guba, M.; Bruns, C. J.; Heeschen, C. Distinct populations of cancer stem cells determine tumor growth and metastatic activity in human pancreatic cancer. *Cell Stem Cell* **2007**, *1*, 313−323.

(14) Wang, D.; Zhu, H.; Zhu, Y.; Liu, Y.; Shen, H.; Yin, R.; Zhang, Z.; Su, Z. CD133(+)/CD44(+)/Oct4(+)/Nestin(+) stem-like cells isolated from Panc-1 cell line may contribute to multi-resistance and metastasis of pancreatic cancer. *Acta Histochem.* **2013**, *115*, 349−356.

(15) Hermann, P. C.; Trabulo, S. M.; Sainz, B., Jr.; Balic, A.; Garcia, E.; Hahn, S. A.; Vandana, M.; Sahoo, S. K.; Tunici, P.; Bakker, A.; Hidalgo, M.; Heeschen, C. Multimodal Treatment Eliminates Cancer Stem Cells and Leads to Long-Term Survival in Primary Human Pancreatic Cancer Tissue Xenografts. *PLoS One* **2013**, *8*, No. e66371.

(16) Lonardo, E.; Hermann, P. C.; Heeschen, C. Pancreatic cancer stem cells - update and future perspectives. *Mol. Oncol.* **2010**, *4*, 431−442.

(17) Lee, C. J.; Dosch, J.; Simeone, D. M. Pancreatic cancer stem cells. *J. Clin. Oncol.* **2008**, *26*, 2806−2812.

(18) Van den Broeck, A.; Gremeaux, L.; Topal, B.; Vankelecom, H. Human pancreatic adenocarcinoma contains a side population resistant to gemcitabine. *BMC Canc.* **2012**, *12*, 354.

(19) Zhou, P.; Li, B.; Liu, F.; Zhang, M.; Wang, Q.; Liu, Y.; Yao, Y.; Li, D. The epithelial to mesenchymal transition (EMT) and cancer stem cells: implication for treatment resistance in pancreatic cancer. *Mol. Canc.* **2017**, *16*, 52.

(20) Ji, J.; Yamashita, T.; Budhu, A.; Forgues, M.; Jia, H.-L.; Li, C.; Deng, C.; Wauthier, E.; Reid, L. M.; Ye, Q.-H.; Qin, L.-X.; Yang, W.; Wang, H.-Y.; Tang, Z.-Y.; Croce, C. M.; Wang, X. W. Identification of microRNA-181 by genome-wide screening as a critical player in EpCAM-positive hepatic cancer stem cells. *Hepatology* **2009**, *50*, 472−480.

(21) Zhang, H. Y.; Li, C. H.; Wang, X. C.; Luo, Y. Q.; Cao, X. D.; Chen, J. J. MiR-199 inhibits EMT and invasion of hepatoma cells through inhibition of Snail expression. *Eur. Rev. Med. Pharmacol. Sci.* **2019**, *23*, 7884−7891.

(22) Zhang, B.; Pan, X.; Cobb, G. P.; Anderson, T. A. microRNAs as oncogenes and tumor suppressors. *Dev. Biol.* **2007**, *302*, 1−12.

(23) Lee, Y. S.; Dutta, A. MicroRNAs in cancer. *Annu. Rev. Pathol.* **2009**, *4*, 199−227.

(24) Khan, A. Q.; Ahmed, E. I.; Elareer, N. R.; Junejo, K.; Steinhoff, M.; Uddin, S., Role of miRNA-Regulated Cancer Stem Cells in the Pathogenesis of Human Malignancies. *Cells* **2019**, *8* (). DOI: 10.3390/cells8080840

(25) Yan, Y.; Zuo, X.; Wei, D. Concise Review: Emerging Role of CD44 in Cancer Stem Cells: A Promising Biomarker and Therapeutic Target. *Stem Cells Transl. Med.* **2015**, *4*, 1033−1043.

(26) Tomita, H.; Tanaka, K.; Tanaka, T.; Hara, A. Aldehyde dehydrogenase 1A1 in stem cells and cancer. *Oncotarget* **2016**, *7*, 11018−11032.

(27) Jeter, C. R.; Yang, T.; Wang, J.; Chao, H.-P.; Tang, D. G. Concise Review: NANOG in Cancer Stem Cells and Tumor Development: An Update and Outstanding Questions. *Stem Cell.* **2015**, *33*, 2381−2390.

(28) Ji, Q.; Hao, X.; Zhang, M.; Tang, W.; Yang, M.; Li, L.; Xiang, D.; Desano, J. T.; Bommer, G. T.; Fan, D.; Fearon, E. R.; Lawrence, T. S.; Xu, L. MicroRNA miR-34 inhibits human pancreatic cancer tumor-initiating cells. *PLoS One* **2009**, *4*, No. e6816.

(29) Agostini, M.; Knight, R. A. miR-34: from bench to bedside. *Oncotarget* **2014**, *5*, 872−881.

(30) Hasegawa, S.; Eguchi, H.; Nagano, H.; Konno, M.; Tomimaru, Y.; Wada, H.; Hama, N.; Kawamoto, K.; Kobayashi, S.; Nishida, N.; Koseki, J.; Nishimura, T.; Gotoh, N.; Ohno, S.; Yabuta, N.; Nojima, H.; Mori, M.; Doki, Y.; Ishii, H. MicroRNA-1246 expression associated with CCNG2-mediated chemoresistance and stemness in pancreatic cancer. *Br. J. Cancer* **2014**, *111*, 1572−1580.
(31) Yang, Z.; Zhao, N.; Cui, J.; Wu, H.; Xiong, J.; Peng, T. Exosomes derived from cancer stem cells of gemcitabine-resistant pancreatic cancer cells enhance drug resistance by delivering miR-210. *Cell. Oncol.* **2020**, *43*, 123−136.
(32) Zhao, H.; Wu, S.; Li, H.; Duan, Q.; Zhang, Z.; Shen, Q.; Wang, C.; Yin, T. ROS/KRAS/AMPK Signaling Contributes to Gemcitabine-Induced Stem-like Cell Properties in Pancreatic Cancer. *Mol. Ther.–Oncolytics* **2019**, *14*, 299−312.
(33) Mani, S. A.; Guo, W.; Liao, M.-J.; Eaton, E. N.; Ayyanan, A.; Zhou, A. Y.; Brooks, M.; Reinhard, F.; Zhang, C. C.; Shipitsin, M.; Campbell, L. L.; Polyak, K.; Brisken, C.; Yang, J.; Weinberg, R. A. The epithelial-mesenchymal transition generates cells with properties of stem cells. *Cell* **2008**, *133*, 704−715.
(34) Morel, A.-P.; Lièvre, M.; Thomas, C.; Hinkal, G.; Ansieau, S.; Puisieux, A. Generation of breast cancer stem cells through epithelial-mesenchymal transition. *PLoS One* **2008**, *3*, No. e2888.
(35) Nomura, A.; Banerjee, S.; Chugh, R.; Dudeja, V.; Yamamoto, M.; Vickers, S. M.; Saluja, A. K. CD133 initiates tumors, induces epithelial-mesenchymal transition and increases metastasis in pancreatic cancer. *Oncotarget* **2015**, *6*, 8313−8322.
(36) Wellner, U.; Schubert, J.; Burk, U. C.; Schmalhofer, O.; Zhu, F.; Sonntag, A.; Waldvogel, B.; Vannier, C.; Darling, D.; Hausen, A. z.; Brunton, V. G.; Morton, J.; Sansom, O.; Schüler, J.; Stemmler, M. P.; Herzberger, C.; Hopt, U.; Keck, T.; Brabletz, S.; Brabletz, T. The EMT-activator ZEB1 promotes tumorigenicity by repressing stemness-inhibiting microRNAs. *Nat. Cell Biol.* **2009**, *11*, 1487−1495.
(37) Su, H.-T.; Weng, C.-C.; Hsiao, P.-J.; Chen, L.-H.; Kuo, T.-L.; Chen, Y.-W.; Kuo, K.-K.; Cheng, K.-H. Stem cell marker nestin is critical for TGF-beta1-mediated tumor progression in pancreatic cancer. *Mol. Cancer Res.* **2013**, *11*, 768−779.
(38) Lamouille, S.; Xu, J.; Derynck, R. Molecular mechanisms of epithelial-mesenchymal transition. *Nat. Rev. Mol. Cell Biol.* **2014**, *15*, 178−196.
(39) Lee, H.-M.; Hwang, K.-A.; Choi, K.-C. Diverse pathways of epithelial mesenchymal transition related with cancer progression and metastasis and potential effects of endocrine disrupting chemicals on epithelial mesenchymal transition process. *Mol. Cell. Endocrinol.* **2017**, *457*, 103−113.
(40) Wang, Y.; Shi, J.; Chai, K.; Ying, X.; Zhou, B. The Role of Snail in EMT and Tumorigenesis. *Curr. Cancer Drug Targets* **2013**, *13*, 963−972.

https://doi.org/10.1021/acsomega.1c02945
ACS Omega 2021, 6, 31435−31446